Synmetamorphic Variscan siderite mineralisation of the Rhenish Massif, Central Europe

ULRICH F. HEIN

Institut für Geologie und Dynamik der Lithosphäre, Goldschmidstr. 3, D-37077 Göttingen, Germany

Abstract

The Rhenohercynian thrust- and fold-belt of Central Europe hosts a syn- to post-kinematic Variscan vein mineralisation, which is restricted to the Rhenish Massif, Germany. It is formed during four major stages and siderite is the principal ore mineral of the 'main stage'. The latter can be traced throughout the massif, but is mainly developed in the Siegerland district as synkinematic lodes which are hosted by low-grade metamorphic pelites of Lower Devonian age.

Fluid inclusion studies prove large-scale homogeneous ore forming fluids of low salinity ($\leq$5 wt.% NaCl equiv.) and Na(–K > –Fe $\gg$ Mg)–Cl composition, which are CO_2 undersaturated (X_{CO_2} = 0.003–0.1). Siderite precipitation at 220–$\leq$320 °C and 0.7–1.4 kbar can be deduced by microthermometry, chlorite themometry, *REE* fractionation and experimental data. Thereby the maximum formation temperature comes close to or even exceeds the peak metamorphic temperature. From Mn contents and $\delta^{13}C$–$\delta^{18}O$ variation of siderite a trend is apparent in which formation temperatures gradually decrease from S.E. to N.W. across the belt. This trend correlates with decreasing degree of host-rock deformation and decreasing metamorphic grade. Fluid composition as well as stable isotopes and *REE* fractionation of siderite point to ore-forming solutions, which were generated and equilibrated at depth during prograde metamorphism.

Structural characteristics of the lodes, age determinations, and *P–T* estimations prove fluid ascent and siderite precipitation during and/or immediately after peak metamorphism predating the postkinematic magmatism of the Rhenohercynian belt. Main(-siderite)-stage mineralisation of the Rhenish Massif is classified as *metamorphogeneous*.

KEYWORDS: siderite, fluid inclusions, *REE* fractionation, Rhemish Massif, Germany.

Introduction

THIS paper presents new data on the Variscan siderite lodes of the Siegerland district, Germany, which have been among the world's largest occurrences of this mineral with a production of 1.75×10^8 t and estimated resources of 0.4×10^8 t. Microthermometric, mineralogical, and geochemical results, in combination with a compilation of published data, permit a better understanding of the ore-forming processes with respect to (1) the *P–T–X* conditions during mineral precipitation, (2) the composition and origin of the ore forming fluids, and (3) the timing of mineralisation in relation to the tectono-metamorphic evolution of the host rocks.

Geological setting

The Rhenohercynian zone of Central Europe is made up of Lower Devonian to Lower Carboniferous rocks. Epicontinental platform sediments with carbonates prevail in the west of the belt (Ardennes Mts), while the eastern basinal areas (Rhenish Massif, Harz Mts) consist of a rock sequence comprising former pelitic sediments, bimodal submarine volcanites and volcaniclastites and reef carbonates (Franke, 1989). Flysch sedimentation starts in Upper Devonian in the southeastern basins and progrades in time towards northwest.

The Rhenohercynian zone represents the external belt of the Variscan orogeny. It is bordered to the north against the autochthonous foreland along the Variscan front. During the Upper Carboniferous the sediments were folded and (due to compressive crustal shortening) stacked along a system of internal listric thrusts (Weber, 1981). In the west of the zone (Belgium, Northern France) the Variscan front is close to the southern margin of the Caledonian London–

Mineralogical Magazine, September 1993, Vol. 57, pp. 451–467

Brabant massif, which acted as a mechanical ramp during deformation, leading to extensive thrusting over the foreland sediments and to a complex imbricate fan along the Faille du Midi (Bois *et al.*, 1988; Bouckaert *et al.*, 1988; Bless *et al.*, 1989). East of the London–Brabant massif, thrusting is less pronounced as overall compression was compensated along a system of submeridional transcurrent faults which extend fan-like from the external belt into the foreland (Franke, 1990; Hofmann, 1990).

The rocks of the Rhenohercynian were affected by prograde metamorphism of lower greenshist facies in a small belt ('phyllite zone', Fig. 1) at the southeastern margin of the zone (Anderle *et al.*, 1990) and in pre-Devonian inliers, such as the

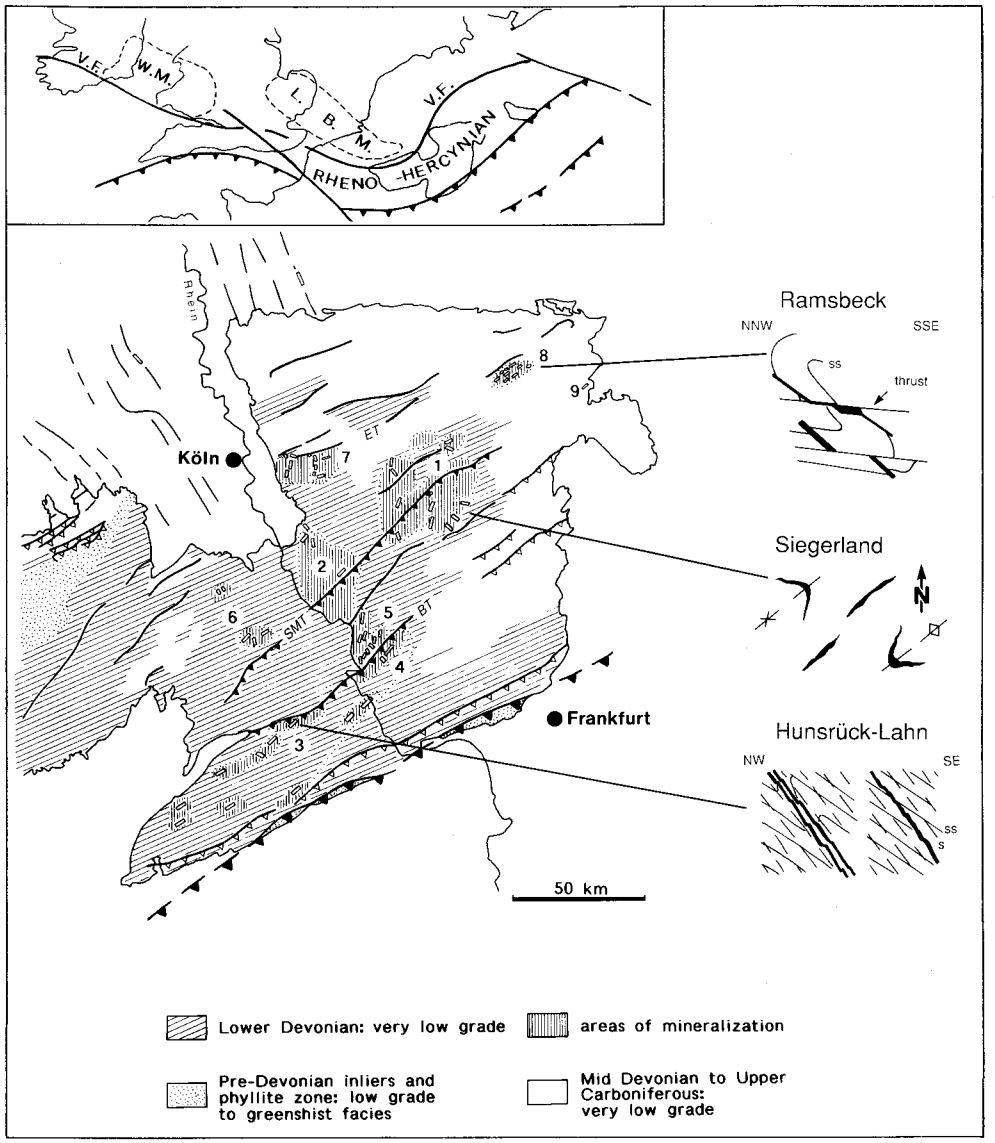

FIG. 1. Distribution and style of synorogenic vein mineralisation in the Rhenish Massif. Numbers refer to mining districts. **Siderite: 1–2** Siegerland–Wied; *Pb–Zn: 3–4* Hunsrück–Lahn, **5** Ems–Braubach, **6** Eifel, **7** Bensberg, **8** Ramsbeck; **Au: 9** Goldhausen. Strike directions of major deposits are indicated by orientation of open rectangles. Major tectonic structures: ***BT*** Boppard Thrust; ***SMT*** Siegen Main Thrust; ***ET*** Ebbe Thurst; **W.M.** Welsh Massif; **L.B.M.** London–Brabant Massif; **V.F.** Variscan front.

Haute Fagne massif of Belgium (Fransolet *et al.*, 1977). The main part of the Rhenohercynian consists of rocks of very low metamorphic grade. The only facies-critical minerals are prehnite–pumpelleyite, observed in paleobasalts, and pyrophyllite in the pelites at a few localities. They define peak metamorphism to maximum temperatures of 300–350 °C and maximum pressures of 2–3 kbar (Meisl, 1970; Weber, 1981) in agreement with studies of coal-rank and illite crystallinity (Oncken, 1987). Metamorphic grade decreases from southeast towards northwest. In the Upper Carboniferous of the Ruhr district, north of the Rhenish Massif (Fig. 1), temperatures were below 200 °C (Buntebarth *et al.*, 1982).

Ore mineralisation

The low-grade metamorphic rocks of the Rhenohercynian belt host a synorogenic vein-type mineralisation, which shows a number of common characteristics over the entire area (Hein and Behr, 1991*b*):

(1) Ore mineralisation is restricted to the Rhenish Massif, Germany (Fig. 1) and is developed along internal shear zones including major structures such as the Boppard Thrust, Siegen Main Thrust, and Ebbe Thrust. Along the northern margin of the massif a few transcurrent faults which extend into the foreland are mineralised (Hein and Behr, 1991*b*; Redecke, 1992). Variscan vein mineralisation is absent in the Ardennes and occurs in only one locality in the Harz Mountains (Lüders and Möller, 1992).

(2) Mineralisation is restricted to host rocks of Lower Devonian age with the exception of the Ramsbeck district, where mineralised veins occur in mid-Devonian shales and quartzites.

(3) Despite local peculiarities the mineralisation shows widely uniform parageneses on a regional scale. Published mineralogical records and our own observations result in a general paragenetic scheme (Fig. 2) which elucidates the temporal and compositional development of the mineralisation during four major stages:

An *early stage* with host-rock silicification and sulphide mineralisation (arsenopyrite, pyrrhotite) is followed by the deposition of siderite (Siegerland type) during a *main stage* and Pb–Zn sulphides (Hunsrück type, Ramsbeck, Bensberg district) during a *late stage*. A final *rejuvenation*

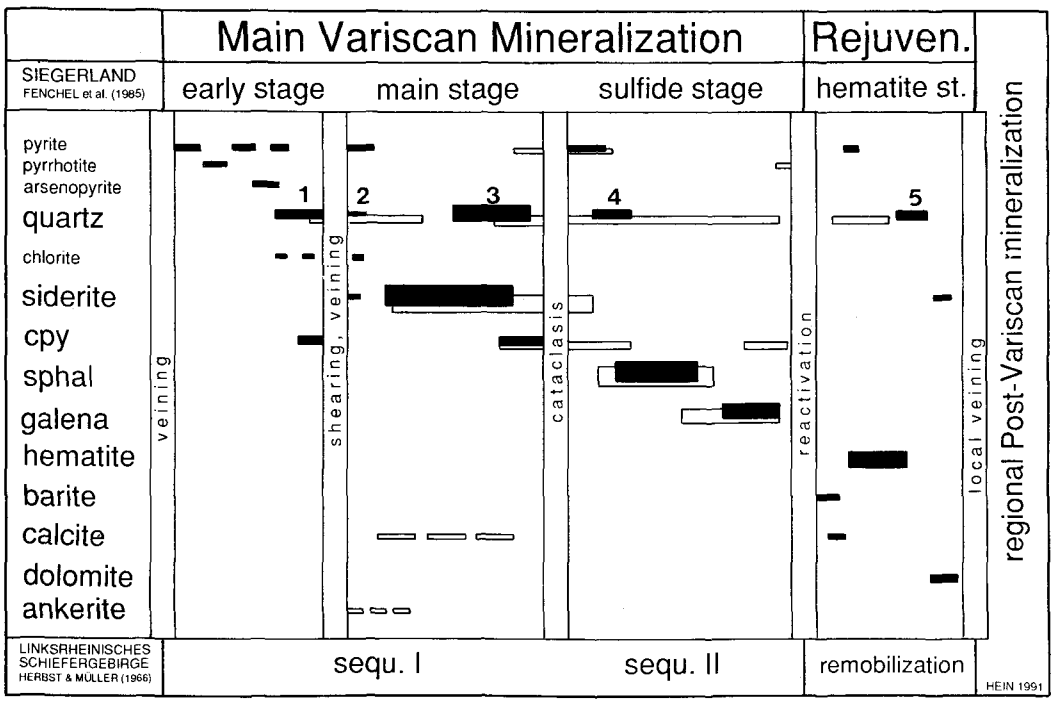

FIG. 2. Generalised paragenetic scheme of the Variscan vein mineralisation of the Rhenish Massif. Compiled after Bauer *et al.* (1979), Fenchel *et al.* (1985), Hannak (1965), Herbst and Müller (1966), Krahn (1988), Lehmann and Pietzner (1970), and own observation.

stage is documented by partial remobilisation or hydrothermal alteration of pre-existing mineralisation. During the last two stages replacement of earlier mineralisation can be locally observed.

This succession is not completely developed at every locality. Moreover, this temporal sequence is also developed as vertical zoning in some Siegerland veins, where sulphides locally occur in the outer parts of the district. Downwards, these veins grade into siderite and at depth into barren quartz (Bornhardt, 1910/12; Walther, 1986).

(4) The mineralised structures of individual mining districts vary in style (Fig. 1) reflecting differences in the age of individual mineralisation stages relative to the age and degree of host-rock deformation.

Early stage mineralisation is minor, but can be traced all over the Rhenish Massif. It is pre- to synkinematic since veins are folded or affected by cleavage-parallel shearing. *Main stage* mineralisation is best developed as siderite lodes in the Siegerland and Wied districts and less important in other districts. The lodes developed during folding of the host rocks in zones of axial ramps from diagonal faults (and subordinately along cross-strike faults) as 'hooked veins' (Walther, 1986). Slatey cleavage is a late element during folding and coincides with mineralisation. On one hand siderite veins are sheared along cleavage planes and on the other hand cleavage-parallel siderite infillings occur. Furthermore, siderite veins are displaced by late Variscan dip-slips (Fenchel *et al.*, 1985). In individual veins early siderite is developed as 'banded spar', i.e. selvage-parallel alternating layers of yellowish and grey siderite. The colour of the 'greyspar' layers results from mylonitic host-rock fragments which document repetitive shearing during veining (Walther, 1986). All observations prove the synkinematic formation of the siderite lodes during the final stage of overall compressive deformation of the host rocks. Ahrendt *et al.* (1983) demonstrated the development of the slatey cleavage to be synchronous with maximum deformation and peak metamorphism, which they have dated at 316 ± 10 (Rb/Sr) and 312 ± 10 Ma (K/Ar) respectively for the central Siegerland district.

Sulphide stage mineralisation follows after a period of cataclasis and is rare in the Siegerland and Wied districts. Major Pb–Zn veins occur parallel to the Rhine valley (Hunsrück-Lahn and Bensberg districts; Fig. 1) and in the northern Rhenish Massif (Ramsbeck district). The veins are paragenetically uniform over the area, but exhibit regional structural differences. Due to the temporal migration of the front of maximum deformation to the north, synkinematic compressive vein structures (ore mylonites and 'flats'; Bauer *et al.*, 1979) exist at Ramsbeck (Fig. 1). They are dated at 305 to 302 ± 10 Ma (K/Ar) and 290 ± 9 Ma (Rb/Sr) respectively (Ahrendt *et al.*, 1983). In the northwestern Bensberg district, extensional structures parallel to cross-strike faults and diagonal faults prevail (Lehmann and Pietzner, 1970). In the southern Rhenish Massif, initial extension after maximum deformation led to late-kinematic veining parallel to the pre-existing cleavage ('cleavage veins'; Hannak, 1964). In all districts, Pb–Zn veins were affected by late-Variscan dip-slip deformation associated with the final stage of folding (Bornhardt, 1910; Walther, 1986).

Rejuvenation stage mineralisation occurs locally in the southern Rhenish Massif as cross-strike veins cross-cutting pre-existing Pb–Zn veins. The similarity of these extensional structures to 'Alpine fissures' was already pointed out by Bornhardt (1910/12). In the central Siegerland the rejuvenation stage started with baryte deposition followed by local hematisation of siderite. Structurally, this stage can be related to the widespread extension during uplift of the Rhenish Massif in late Upper Carboniferous/Early Permian (Oncken, 1993).

Sampling and analytical procedure

Although mining is abandoned, exactly localised specimens of defined paragenesis were available from collections of the Technical University, Clausthal, the Federal Institute of Geosciences, Hannover, the Mineralogical Museums of Göttingen and Marburg, and a number of private collections. The samples cover the siderite stage of the Rhenish Massif (Fig. 1) and, for a few mines, the full vertical extension of the mineralisation (>1200 m).

Fluid inclusions studies were performed at the Institute of Geology and Dynamics of the Lithosphere, Göttingen using a Linkam THM 600 heating- and freezing-stage, which was calibrated by synthetic fluid inclusions (SYNFLINC) (Heinrich *et al.*, 1992). A Ramanor U-1000 served for routine Raman analyses of the gas phases. Time-integrating Fourier-transform Infrared spectroscopy (FTIR) was done as bulk analysis of fluid inclusion from 40 × 40 μm sections using a 1760 × Perkin-Elmer Spectrometer. This permits the qualitative detection of smallest quantities of CO_2 and H_2O down to 0.03 mole % even in inclusions, which are not accessible by microthermometry because of size.

Chlorites and carbonates were analysed for

their main elements with an EDX system on a Cambridge Instruments SEM (Stereoscan 250 MK3) using pure Co and Kakanui pyroxene as standards. For comparison, some samples were cross-checked by electron microbe at the Mineralogical Institute, Aachen, using an ARL–SEMQ. The reproducibility of both analyses is within the analytical error, which is typically better than ±2% relative.

Rare-earth elements (*REE*) of hand-picked siderite were analysed at the Hahn–Meitner Institute, Berlin, using a Perkin-Elmer/Sciex ICP–MS. Analytical details are given by Dulski (1992). Stable isotope analyses of the same siderite samples (C,O) were undertaken at the Geochemical Institute, Göttingen. Analytical details are given by Zheng (1991).

Microthermometry

Fluid inclusions were studied in main-stage quartz and siderite from the Siegerland district, the Ramsbeck Pb–Zn deposit, the Ems–Braubach district, the Hunsrück–Lahn district and additionally in quartz from synkinematic barren veins and segregations. The following data result from the study of approximately 1400 inclusions, including measurements of Erlinghagen (1989). Only those inclusions which are considered as primary or early—as verified by petrographic studies—and which represent entrapment during the siderite stage are referred to. Some samples were studied by optical as well as SEM-cathodoluminescence to exclude hydrothermal overprint during the successive stages of mineralisation.

Most of the fluid inclusions appear as two-phase aqueous inclusions (LV-type) at room temperature. More than 90% of the inclusions reveal initial melting temperatures (*Te*) above −21 °C and point to entrapment of Na(–K)–Cl-dominated aqueous solutions. The *Te* of a few inclusions range down to −35 °C indicating the presence of additional cations. K, minor Fe, and rare Mg were verified in addition to Na by analysing evaporates of opened inclusions with SEM–EDX. These results are in agreement with the neutron activation analyses of Gerler (1990) who reports element wt. ratios of K/Na = 0.09–0.18 and Fe/Na = 0.08–0.40 for siderite-stage fluids. Ice melting is the only phase transition visible at low temperatures besides intial melting. There is no evidence of hydrate melting above *Te*. The homogenisation temperatures (*Th*) are slightly higher for the Hunsrück–Lahn district (up to 300 °C) in comparison with the Siegerland siderite lodes (170–250 °C). Salinites are generally low for the siderite-stage fluid inclusions ($Tm_{ice} \geqslant$ −7 °C) and do not vary significantly with the *Th*. On the other hand, fluid inclusions trapped during the later sulphide stage show increasing salinities with falling total homogenisation temperatures (Fig. 3). The data of barren quartz veins along the major thrust show a similar variation. Fluid inclusions showing variable *Th* and identical Tm_{ice} indicate density variation along the thrusts.

Three-phase H_2O–CO_2 inclusions (LLV-type) with aqueous solution, vapour, and an extremely narrow rim of liquid CO_2, just visible at room temperature, are rare. In a few inclusions, partial homogenisation of the CO_2 phase to liquid is observed close to the critical temperature (+31 °C). In many quartz samples, tiny monophase gas inclusions of low density can be observed. Furthermore, in a number of two-phase aqueous inclusions (LV-type) gas condensation becomes visible on cooling. These inclusions only rarely permit exact microthermometric measurements, but studies by time-integrating FTIR qualitatively proves small quantities of CO_2 to be a common constituent besides water (Fig. 4). Other gas species could not be identified by Raman spectroscopy. As a fluid phase should occupy a minimum of 10 vol.% of an inclusion to be visible at room temperature (Walther, 1981), the combination of microthermometric observation and the detection limit of FTIR permits an overall estimation of the composition of the H_2O–CO_2 inclusions in the range of $0.003 \geqslant X_{CO_2} \geqslant 0.1$.

Erlinghagen (1989) reports 'primary' three phase inclusions (LLV) in siderite and quartz 3 (Fig. 2) with a CO_2-phase of about critical density from three Siegerland mines (Stahlberg, Apollo, Neue Haardt; for individual localities compare Fenchel *et al.*, 1985, and Walther, 1986). A petrographic reinvestigation of his samples shows that these inclusions occur only where siderite is partly replaced by quartz 4 of the succeeding sulphide stage. Furthermore, Erlinghagen (1989) reports primary inclusions of equal CO_2 density in quartz 4 and sphalerite of the Stahlberg mine. Therefore, his LLV inclusions in siderite are reinterpreted as either being trapped or reequilibrated during the sulphide stage.

Chlorite thermometry

Chlorite is a common gangue mineral besides quartz and rare illite/sericite and occurs during the early stage and the following main(-siderite) stage. A set of 48 vein chlorites from the southern Rhenish Massif (Hunsrück–Lahn district) represents ore deposits as well as barren quartz mineralisation along the Boppard thrust. In these

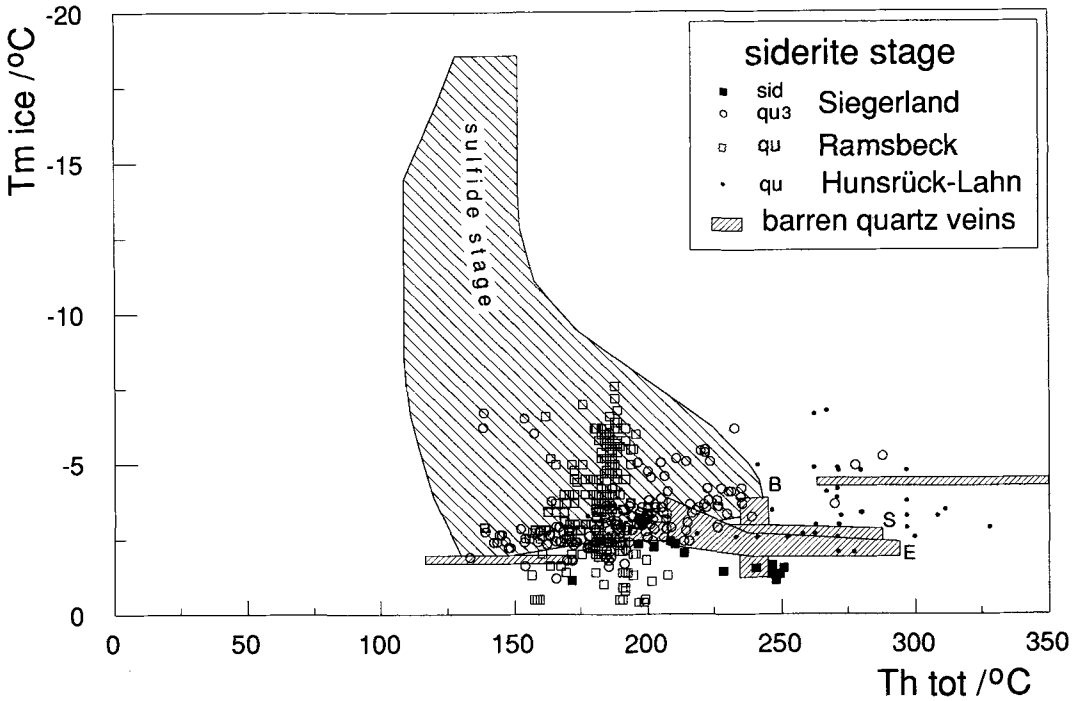

FIG. 3. Tm_{ice}-Th-variation of siderite stage fluid inclusions of various localities (**B** Boppard Thrust; **S** Siegen Thrust; **E** Ebbe Thrust). The trend of fluid development during the succeeding sulphide stage (hatched area) is given for comparison.

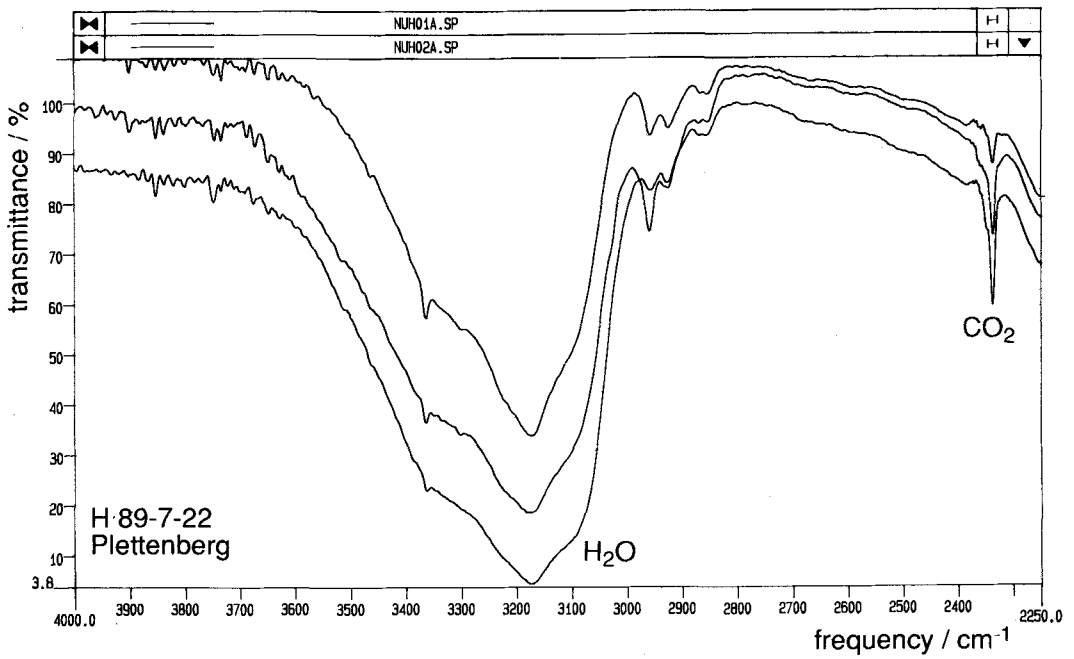

FIG. 4. FTIR spectra of fluid inclusions in three 40 × 40 μm sections of an individual quartz sample from Plettenberg, Rhenish Massif. Upper and lower curve are graphically shifted for better distinction.

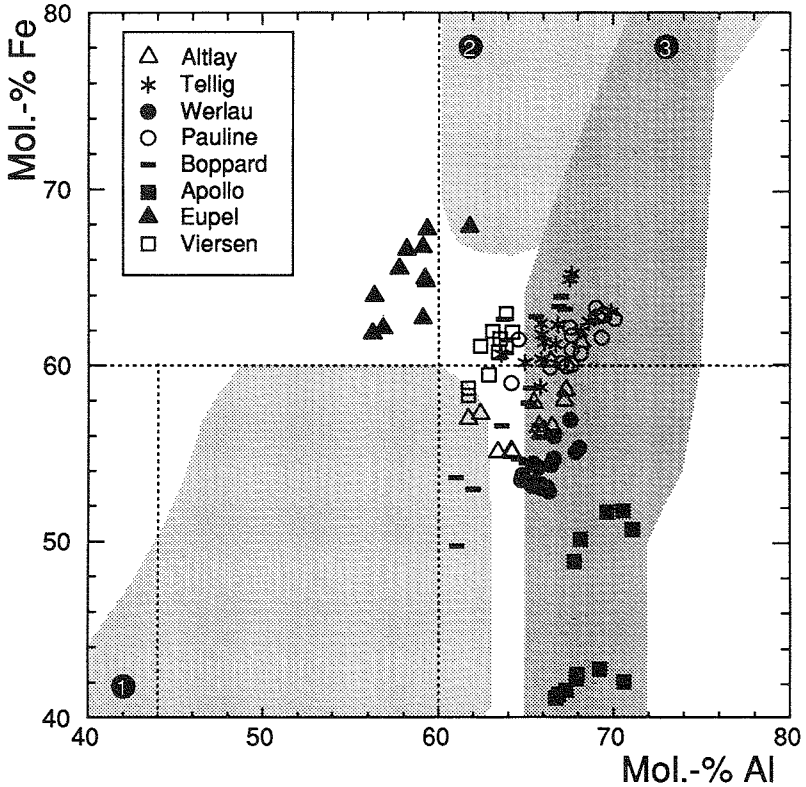

FIG. 5. Composition of vein chlorites of different localities after the classification of Tröger and Trochim (1966). Chlorite composition of (1) spilitic rocks, Lahn syncline (Eyssen, 1985), (2) exhalative hematite ores, Lahn syncline (Eyssen, 1985), and (3) footwall alteration halo, Rammelsberg deposit, Harz Mountains (Käselitz, 1988) is given for comparison (dotted patterns).

samples chlorite predates Fe–Mn-carbonates. Two chlorite samples, both intimately intergrown with siderite, are from the Siegerland district (Eupel, Apollo).

Following the classification scheme of Tröger and Trochim (1966), the samples proved to be orthochlorites of ripidolitic to aphrosideritic composition (Fig 5), and one sample is classified as brunsvigite/chamosite. The composition of hydrothermal chlorite of genetically different ore-mineralisation of the Rhenohercynian belt is given for comparison in Fig. 5, i.e. (1) the footwall alteration halo of the SEDEX-type Rammelsberg massive sulphide deposit, Harz Mts (Käselitz, 1988) and (2) chlorite in hematite ores and diabases resulting from spilitisation of paleobasalts (Eyssen, 1985).

Vein chlorite compositions are close to those from the Rammelsberg deposit. Similar compositions are reported by Vogtmann-Becker (1990) from barren quartz–carbonate veins and Cambro-Ordovician host rocks of the Stavelot–Fagne Massif and by Redecke (1992) from mineralised Variscan transcurrent faults in the underground of the Niederrheinische Bucht (Köln–Aachen area; Fig. 1). The Fe/(Fe + Mg) ratios of vein chlorites from the southern Rhenish Massif vary between 0.55 and 0.72, which is close to Fe/(Fe + Mg) ratios of the Lower Devonian pelitic host rocks (0.60–0.70; Schulz–Dobrick and Wedepohl, 1983). The composition of these chlorites are assumed to reflect fluid–rock equilibrium.

Chlorite composition is dependent on T, f_{O_2}, and f_S (Walshe, 1986) and can be used to estimate formation temperatures at a given fluid composition. Three published thermometers (Cathelineau and Nieva, 1985; Walshe, 1986; revised calibration of Cathelineau, 1988) have applied to the samples. The results (Table 1) show acceptable agreement for two thermometers (Cathelineau and Nieva, 1985; Walshe, 1986), while the third one (Cathelineau, 1988) models temperatures which are about 50–70 °C above. The latter

Table 1: Vein chlorite: Comparison of different thermometers (1–5) and calculated minimum pressures of formation

sample	locality	1 T / °C	2 T / °C	3 T / °C	4 T / °C	5 T / °C	6 P / bar
H 89-6-30	Altlay	214 - 230	277 - 300	280 - 305	335 - 377	342 - 385	1010-1063
H 89-6-32A	Tellig	205 - 245	288 - 316	288 - 316	347 - 361	355 - 369	1025-1365
H 89-6-10	Pauline	260 - 300	290 - 318	278 - 310	334 - 384	339 - 392	(277-437)
H 89-7-27	Braubach	-	279 - 297	287 - 301	348 - 370	357 - 379	-
H 89-7-28	Braubach	235 - 241	-	280 - 294	331 - 361	336 - 368	681-783
H 51	Apollo	180 - 230	292 - 331	300 - 333	367 - 417	369 - 422	(1474-1933)
H 588	Eupel	-	220 - 247	256 - 269	301 - 331	309 - 329	-

Thermometers: 1.: Microthermometry ; 2. Walshe, 1986; 3. Cathelineau & Nieva, 1985; 4. Cathelineau, 1988; 5: Jowett (1991). 6: For pressure calculation see text.

are slightly shifted to even higher temperatures by applying the correction proposed by Jowett (1991).

Despite analytical restrictions (no independent Fe^{3+} or H_2O determination, and idealised formulae) the model temperatures may be accepted as representing the range of chlorite formation (Bennett and Barker, 1992), although some temperatures after Cathelineau (1988) seem to be too high from a geological/petrological viewpoint. Consequently, the Walshe–thermometer is accepted to represent minimum temperatures which are close to or even above the peak metamorphic temperature of the Rhenish Massif.

Siderite geochemistry

Manganese content. Siegerland siderite contains Mn in the percent range. Throughout the active mining period, numerous analyses were carried out, which have been summarised for individual deposits and districts by Wettig (1974) and Walther (1986). Detailed studies of Hannak (1965) and Hannak and Gundlach (1967) prove the molar ratios of Fe, Mn, Ca, and Mg to be constant within individual districts, i.e. tectonometamorphic units, even over large distances (>80 km). Furthermore, they indicate no significant main-element variation with depth. Present microprobe analyses of the siderite main-element composition fit into the ranges reported by the above authors.

Fig. 6 summarises the average values of the individual mining districts of the Rhenish Massif. The Mn-contents of siderites (expressed as Fe/Mn ratios in Fig. 6) increase systematically (up to 10 mol.%) from N.W. (Bensberg district) to S.E. (Hunsrück–Lahn district) except siderite from the Ems–Braubach district immediately north of the Boppard Thrust. According to Schulz-Dobrick and Wedepohl (1983) regionally increasing Mn-contents are not found for the Lower Devonian pelitic host-rocks of the individual districts. Therefore, the Mn-trend of siderite must be independent of the host-rock composition.

Rare-earth elements (REE). REE distribution patterns can assist in genetic interpretation of carbonate minerals (Möller, 1983; Bau and Möller, 1992). 33 siderite samples from the major mining districts across the Rhenish Massif (Bensberg, Siegerland, Hunsrück; Fig. 1) have been analysed for their *REE* contents (Table 2). The distribution patterns discussed here are normalised to 'European shale', which stands for the average composition of the European continental crust (Haskin and Haskin, 1966), since mineralisation is regarded as a process of intracrustal element redistribution.

The *REE* distribution patterns of siderite are similar at a given deposit. The Füsseberg mine (Siegerland district) serves as an example (Fig. 7), where *REE* signatures are nearly identical over a depth of 500 m down the mineralised structure. Even over the entire area, the patterns are similar for most of the samples. They exhibit little fractionation of the *HREE* (Fig. 8), the contents of which are one magnitude above those of the *LREE*, which are additionally fractionated. The *REE* contents of a carbonate are controlled by the *REE* content of the mineralising fluid, the *REE* distribution between the fluid and the precipitating mineral, and the size of sites available for *REE* incorporation into the lattice (Möller, 1983). As the effective ionic radii of *LREE* differ more from that of Fe^{2+} than those of *HREE*, the latter are preferentially incorporated into siderite (see discussion in Bau, 1991). Therefore, the above distinct fractionation between *LREE* and *HREE* is mainly caused by 'crystallographic control' (Morgan and Wandles, 1980).

The similarity of the patterns is taken as indicative of siderite precipitation from a large-scale uniform fluid system. The only differences in patterns relate to the Eu-contents and permit the distinction of three subtypes (Fig. 8). While most patterns show no anomaly, a few samples from the Siegerland district are characterised by

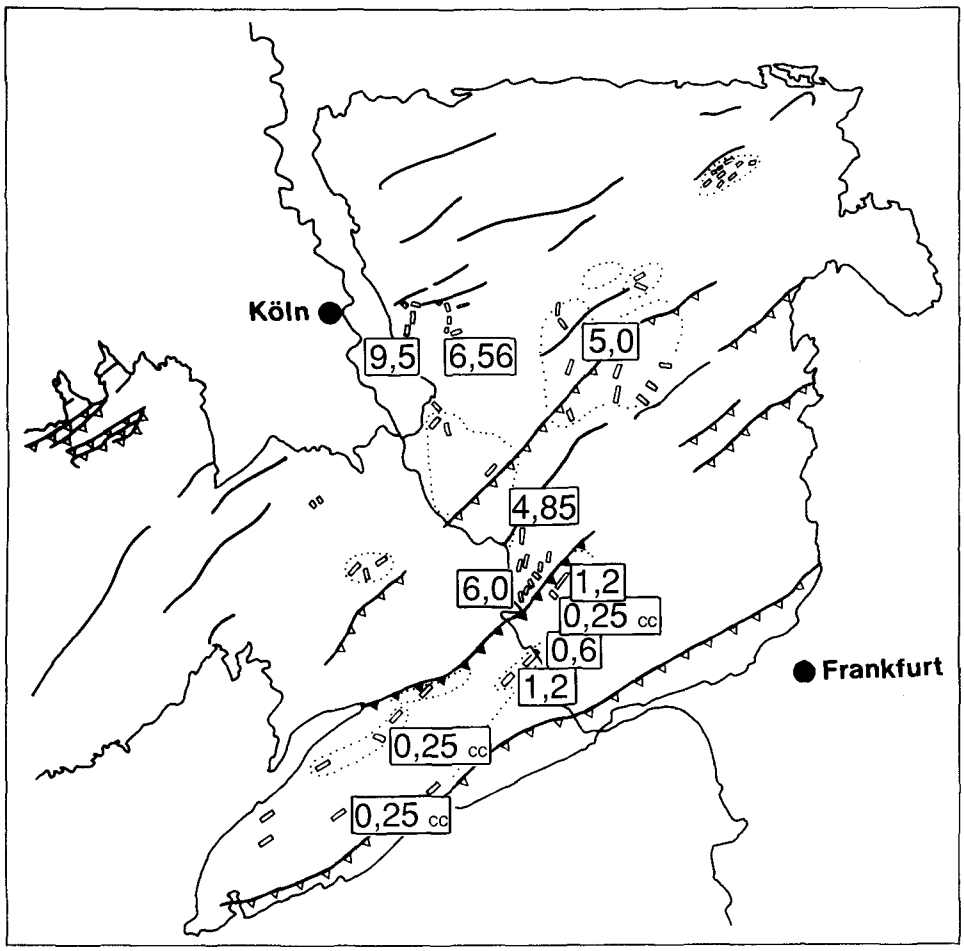

FIG. 6. Average Fe/Mn ratios of siderite and main-stage calcite (cc) in individual mining districts of the Rhenish Massif. For tectonic structures compare Fig. 1.

slightly negative Eu-anomalies. Positive Eu-anomalies are restricted to samples from the southeastern Hunsrück–Lahn district and a few localities of the Siegerland (see discussion).

Stable isotopes. Stable isotopes (C–O) of the same siderite samples which served for *REE* determination have been analysed (Table 2). With one exception, $\delta^{13}C$ and $\delta^{18}O$ exhibit a very limited variation for a given deposit. In one case (Eisenzecherzug mine) the variation is within the analytical error even over a depth of 800 m. Isotope compositions of Siegerland siderite cover the range reported by Stahl (1971: $\delta^{13}C_{PDB}$ = −11.6 to −8.3‰, $\delta^{18}O_{SMOW}$ = 16.4 to 19.1‰) for eight Siegerland samples.

In a $\delta^{13}C$–$\delta^{18}O$ variation diagram, the isotope compositions of individual districts plot into different clusters (Fig. 9). By regional-scale consideration of all data a positive correlation is apparent: $\delta^{13}C$ and $\delta^{18}O$ increase systematically from Southeast (Hunsrück–Lahn district) to Northwest (Bensberg district) across the Rhenish Massif. The overall $\delta^{13}C_{PDB}$-variation of siderites is small (−12 to −9‰) whereas $\delta^{18}O_{SMOW}$-variation (+11.5 to +20‰) is more pronounced. The correlation is not perfect and the slight $\delta^{13}C_{PDB}$-variation indicates the possible presence of another carbon species besides CO_2.

On a more local scale, similar $\delta^{13}C_{PDB}$ correlation of siderite is reported by Zak and Dobes (1991) for the Variscan vein deposits at Pribam, CSFR, and by Zheng (1991) for the Post-Variscan vein-district of the Upper Harz Mountains, Germany (Fig. 9).

Table 2: REE contents and stable isotope composition of vein siderites from individual mining districts of the Rhenish Massif. (REE in ppm; $\delta^{13}C$ and $\delta^{18}O$ in %; n.a.= not analyzed.)

sample	locality	La	Ce	Pr	Nd	Sm	Eu	Gd	Tb	Dy	Ho	Er	Tm	Yb	Lu	$\delta^{13}C_{PDB}$	$\delta^{18}O_{SMOW}$
Siegerland district																	
H 41/84	Pfann	0.03	0.19	0.03	0.24	0.52	0.27	1.50	0.43	2.57	0.51	1.46	0.24	1.54	0.20	-11.26	15.38
H 586/85	Anxbach	0.45	1.58	0.29	1.90	1.58	0.50	2.49	0.50	2.40	0.39	0.86	0.10	0.57	0.07	-10.74	14.97
H 587/85	Eupel	0.16	0.37	0.33	3.24	4.45	2.12	5.49	0.71	2.50	0.34	0.65	0.07	0.44	0.05	-10.05	15.98
H 588/85	Eupel	0.06	0.28	0.08	0.72	0.92	0.30	1.51	0.30	1.54	0.26	0.67	0.09	0.59	0.08	-9.97	16.56
H 591/85	Eisenzech	1.31	2.11	0.23	1.02	0.43	0.13	0.75	0.20	1.35	0.31	1.10	0.23	2.21	0.36	-11.58	14.67
H 593/85	Eisenzech	0.22	0.48	0.08	0.49	0.44	0.16	0.96	0.28	1.98	0.48	1.58	0.31	2.60	0.35	-11.00	14.96
H 594/85	Eisenzech	0.22	0.51	0.07	0.50	0.39	0.14	0.84	0.21	1.51	0.35	1.28	0.27	2.41	0.38	-11.49	14.68
H 596/85	Georg	0.07	0.09	0.02	0.16	0.20	0.14	0.38	0.10	0.54	0.12	0.39	0.08	0.72	0.11	-11.17	16.26
H 598/85	Georg	1.48	2.73	0.28	1.28	1.84	1.76	5.80	1.28	6.28	0.94	2.18	0.29	1.87	0.25	-11.69	17.47
H 618/85	Vereinigung	0.09	0.79	0.26	2.81	3.99	0.91	5.76	0.96	4.62	0.80	1.98	0.26	1.76	0.23	-10.21	15.41
H 635/85	Pfann	0.08	0.46	0.05	0.41	0.39	0.13	0.75	0.21	1.67	0.41	1.63	0.35	3.39	0.50	-11.20	15.66
H 637/85	Herdorf	0.18	0.62	0.09	0.63	0.87	0.62	1.52	0.32	1.57	0.25	0.58	0.07	0.46	0.05	-11.59	14.02
H 639/85	Füsseberg	0.14	0.4	0.07	0.48	0.43	0.11	0.88	0.32	2.54	0.69	2.6	0.54	4.45	0.57	-11.26	14.70
H 640/85	Füsseberg	0.04	0.64	0.05	0.56	0.63	0.20	1.21	0.39	2.29	0.48	1.34	0.19	1.19	0.14	-11.51	14.78
H 641/85	Füsseberg	0.17	1.42	0.26	2.00	1.58	0.28	2.70	0.74	4.32	0.87	2.69	0.43	2.87	0.37	-10.93	15.36
H 643/85	Füsseberg	0.08	0.39	0.10	0.83	0.90	0.25	1.74	0.50	3.42	0.67	1.83	0.24	1.31	0.15	-11.20	16.23
H 644/85	Füsseberg	0.15	0.81	0.21	1.69	1.73	0.33	2.73	0.65	4.05	0.76	2.23	0.38	3.10	0.44	-10.98	16.12
H 645/85	Füsseberg	0.30	1.41	0.36	3.19	2.86	0.39	4.00	0.79	4.93	0.97	2.90	0.50	3.57	0.49	n.a.	n.a.
Southern Lahn district																	
H 89-6-4	Holzappel	4.07	10.80	1.52	7.86	3.30	2.91	4.02	0.65	3.63	0.65	1.72	0.20	1.18	0.15	-11.84	12.65
H 89-6-5	Holzappel	0.40	1.99	0.55	5.04	6.42	3.20	9.00	1.58	7.97	1.39	3.45	0.44	2.70	0.37	-11.42	11.93
H 89-6-13	Werlau	2.76	13.70	2.95	18.40	7.50	7.59	6.89	0.75	3.11	0.48	0.99	0.10	0.56	0.08	-11.21	11.85
H 89-6-14	Werlau	1.66	7.40	1.65	11.30	6.72	5.15	7.48	1.07	5.33	0.93	2.13	0.24	1.35	0.18	-11.11	11.96
H 89-6-15	Werlau	0.36	2.41	0.75	6.49	5.56	5.21	7.98	1.21	6.13	1.04	2.44	0.27	1.39	0.18	-11.16	11.61
Northern Lahn district																	
H 89-6-1	Rosenberg	0.21	0.99	0.26	2.51	3.35	1.27	4.50	0.75	3.56	0.54	1.19	0.15	0.97	0.14	-9.43	16.41
H 89-6-2	Rosenberg	0.43	4.19	0.72	7.25	9.14	3.85	10.80	1.58	7.04	1.10	2.70	0.35	2.26	0.32	-9.18	16.34
H900328-14	Bad Ems	0.17	0.44	0.08	0.58	0.88	0.92	2.23	0.51	2.88	0.48	1.29	0.18	1.26	0.17	-9.58	17.16
Eifel district																	
Katz-1	Katzbach	0.24	1.84	0.66	6.40	6.76	2.23	7.69	1.24	6.06	1.01	2.34	0.30	1.82	0.21	n.a.	n.a.
Ben-1	Bendisberg	0.02	0.16	0.05	0.61	1.27	0.49	2.01	0.44	2.34	0.40	1.06	0.17	1.14	0.15	n.a.	n.a.
Sil-1	Silbersand	0.03	0.17	0.05	0.46	0.89	0.41	2.82	0.62	3.33	0.53	1.26	0.17	1.09	0.14	n.a.	n.a.
Saa-1	Saarsegen	0.10	0.86	0.28	2.58	5.00	1.99	11.60	2.31	12.40	2.15	5.31	0.75	4.91	0.67	n.a.	n.a.
Bensberg district																	
H 577/85	Nic. Phön.	0.06	4.08	0.07	0.73	1.51	0.62	4.01	0.82	4.41	0.73	1.73	0.21	1.16	0.15	-10.74	15.75
H 578/85	Nic. Phön.	0.05	0.25	0.06	0.62	1.34	0.52	3.59	0.79	4.29	0.73	1.71	0.22	1.32	0.17	-10.60	19.11

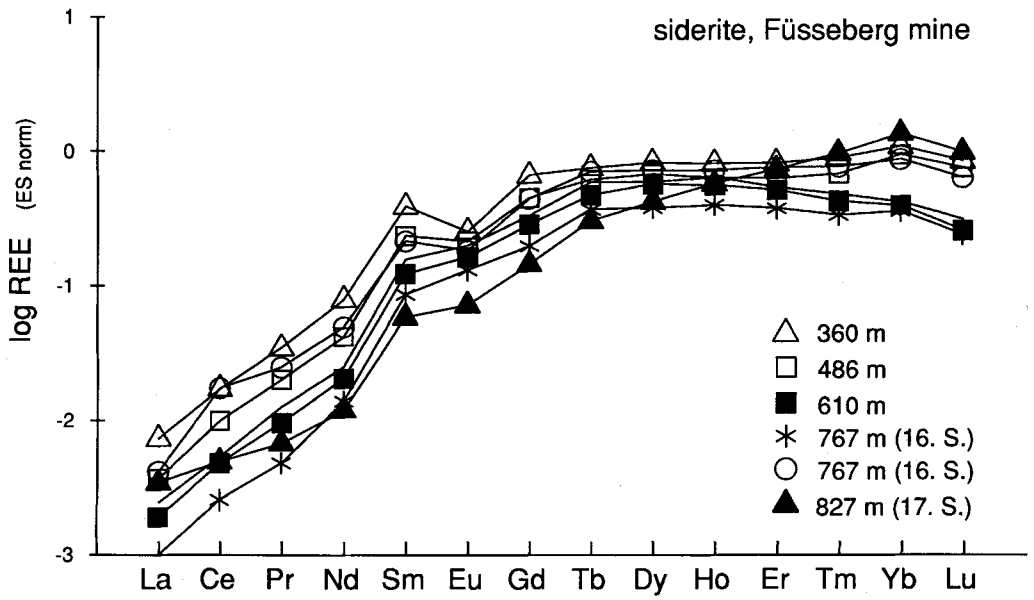

FIG. 7. ES-normalised *REE* distribution patterns of siderite from different levels of the Füsseberg mine, Siegerland district.

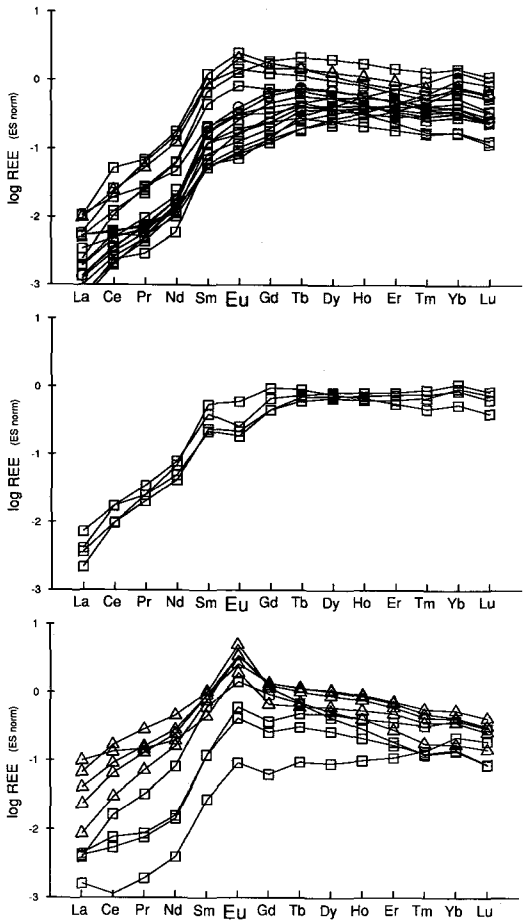

FIG. 8. ES-normalised *REE* distribution patterns of siderite from different mining districts of the Rhenish Massif. Subdivision according to Eu anomalies and independent of localities (triangles: Hunsrück–Lahn; squares: Siegerland and Eifel; circles: Bensberg).

Discussion

P–T–X conditions of siderite precipitation. Combined application of microthermometry, Raman analysis and FTIR spectrometry proves siderite precipitation from CO_2-undersaturated aqueous Na(–K>–Fe≫–Mg)–Cl solutions of low salinity (≤5 wt.% NaCl equiv.) at temperatures above 180–250 °C for the Siegerland district. For the veins of the Hunsrück–Lahn area the minimum formation temperatures extend to 300 °C.

Experimental data on the hydrothermal stability of siderite and thermodynamic properties are limited. French (1971) reports experiments in the system Fe–C–O and Frost (1979*a*) discusses the stability of siderite in a C–O–H fluid phase. Siderite stability is limited as a function of f_{O_2} and temperature (Fig. 10) by oxidation to hematite or decomposition to magnetite or magnetite + graphite. Stability limits approximate the HM– and graphite-buffer respectively. Moreover, the siderite–magnetite equilibrium depends on X_{CO_2} of the fluid phase (Schwartz and Suronjo, 1990). The estimated X_{CO_2} = 0.003–0.1 of the siderite-stage fluids delimits the possible formation temperatures in the range of 220 °C ≤ T ≤ 300 °C, along the HM-buffer (Fig. 10). The experiments of French (1971) concern pure siderite and lead to disagreements with naturally observed parageneses (e.g. grunerite–siderite in metamorphosed banded Mn-formation) as pointed out by Frost (1979*b*). On the other hand, additional Mn in the system Fe–C–O would shift the stability limits of siderite towards higher f_{O_2} and temperatures as well (French, 1971). Since Variscan siderite of the Rhenish Massif contains Mn in the percent range, higher formation temperatures than 300 °C can be expected.

A similar range of formation temperature can be calculated from the stable isotope data: siderite is the only carbon-bearing phase of the main-stage mineralisation, which excludes the use of isotopic fractionation between cogenetic carbon-bearing minerals as a geothermometer. Fractionation of carbon isotopes between dissolved carbon aqueous species and siderite, as well as fractionation of oxygen isotopes between hydrothermal fluid and siderite are temperature dependent. Fluid inclusions and *REE* fractionation of siderite point to a large scale fluid system of constant composition. By assuming transport of carbon and oxygen in (and co-precipitation as siderite from) one solution, Zak and Dobes (1991) and Zheng (1991) interpret the positive $\delta^{13}C$–$\delta^{18}O$ correlation as a decrease of formation temperatures. Applying this interpretation to siderites of the Rhenish Massif results in formation temperatures which gradually decrease from S.E. (Hunsrück–Lahn district) to N.W. (Bensberg district). This trend of decreasing formation temperatures also correlates with decreasing Mn-contents of siderite (see below).

The range of formation temperature is best expressed by the $\delta^{18}O$-variation as the ore-forming fluid is water-dominated. By assuming an average composition of siderite from the Hunsrück–Lahn district of $\delta^{18}O_{SMOW} \geq +12‰$ (Fig. 9) and a formation temperature of 300 °C, the oxygen isotope composition of the fluid is calculated to be $\delta^{18}O_{H_2O} \approx +8‰$. This fluid composition and a siderite composition of $\delta^{18}O_{SMOW} \geq +17‰$ for the Bensberg district results in T = 230 °C as lower limit of the range of siderite formation temperature. This means a difference

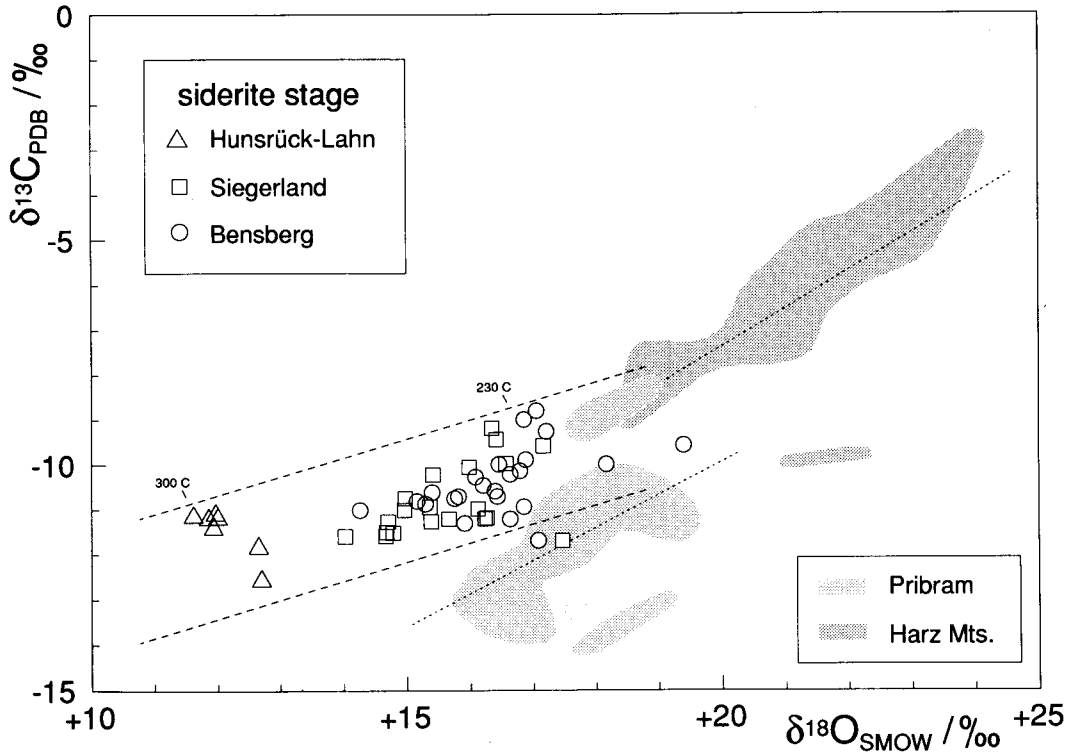

FIG. 9. $\delta^{13}C_{PDB}$-$\delta^{18}O_{SMOW}$-variation of Variscan vein siderite from different mining districts of the Rhenish Massif (18 points after Jux, 1982, included). Dotted patterns for Pribram, CSFR (Zak and Dobes, 1991) and Upper Harz Mountains, Germany (Zheng, 1991) for comparison.

of only 70 °C over a distance of 100–120 km across the belt, when the size of the investigated area is taken into consideration.

Indirectly, a temperature indication is also available from *REE* distribution patterns of siderite. In Fig. 10 the redox equilibrium for Eu^{3+}–Eu^{2+} (1 kbar; pH = 3, i.e. slightly acid; Bau, 1991) is given as function of f_{O_2} and temperature. It becomes apparent that siderite plots in the field of (reduced) Eu^{2+} for temperatures above *c.* 200 °C. Distribution patterns of most studied samples do not show Eu anomalies. As *REE* incorporation is dictated by 'crystallographic control', sorption of *REE* during fluid–rock interaction can be ignored. The slightly positive Eu anomaly of a few siderites from the Hunsrück–Lahn area would point to precipitation below *c.* 200 °C, in disagreement with the temperatures estimates given above. On the other hand, these samples are among the Mn-richest with stability limits shifted towards higher f_{O_2} (i.e. towards the field of Eu^{3+}). This is assumed to explain their positive Eu anomaly at temperatures far above 200 °C.

The uniform parageneses of the Variscan vein mineralisation indicate a decrease in temperature from the early stage of mineralisation to the main-(siderite-) stage (Fig. 2). The lower limit of (early stage) chlorite formation temperatures after Walshe (1986) roughly terminates siderite precipitation below *c.* 300–330 °C. Corresponding pressures (Table 1) have been obtained from the intercept of chlorite temperature and isochores calculated for fluid inclusions in cogenetic quartz of the same samples. They are in the range of 0.7–1.4 kbar.

Fluid origin. The Siegerland siderite lodes have been genetically related to a hypothetic pluton and later to a hidden, deep-seated (>29 km) batholith (Fenchel *et al.*, 1985). However, deep seismic profiles do not give any indication of the existence of a pluton (Franke *et al.*, 1990) and a magnetic anomaly of unknown origin serves as the only argument for a batholith of unknown composition.

The veins are synkinematic as documented by the coincidence of vein-filling and developing of the slatey cleavage (Walther, 1986), which is

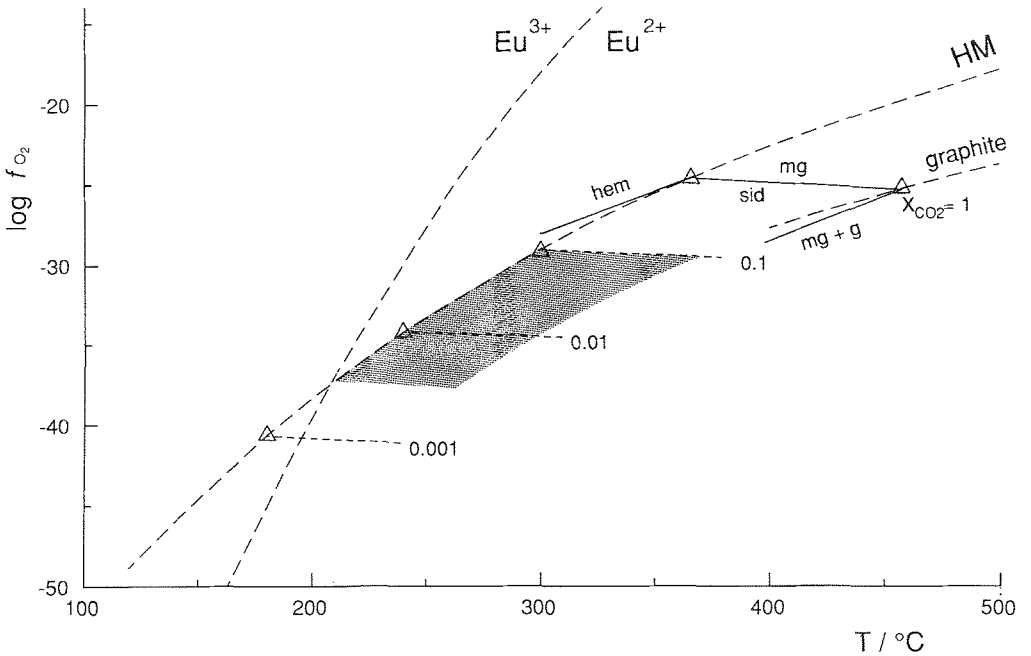

FIG. 10. Stability of siderite in the system Fe–C–O–H after French (1971). Redox equilibrium for Eu^{3+}–Eu^{2+} (1 kbar; pH = 3) after Bau (1991). Siderite–magnetite as function of X_{CO_2} after Schwartz and Suronjo (1990). Dotted field gives limits for vein siderites according to estimated X_{CO_2} (see text).

dated at 316 ± 10 Ma (K/Ar) and 310 ± 10 Ma (Rb/Sr) respectively (Ahrent *et al.*, 1983) in the Siegerland district. Therefore, siderite vein mineralisation predates the post-kinematic acid plutonism of the Rhenohercynian belt. Plutonism is unknown in the Rhenish Massif and restricted to the Harz Mountains. The only indications for basic magmatism are late 'diabase dykes' of unknown age, which cut siderite veins at a few localities (Fenchel *et al.*, 1985).

By isotope (Stahl, 1971) and fluid inclusion studies (Erlinghagen, 1989) siderite has been classifed 'mesothermal', being precipitated from 'magmatic-hydrothermal' ore-forming solutions. Both studies concern samples from the Siegerland district only. Present fluid inclusion studies prove CO_2-undersaturated aqueous Na(–K>–Fe≫–Mg)–Cl fluids as ore-forming solutions of the siderite stage. This fluid composition is typical for the metamorphic Variscan basement of Central Europe (Behr, 1989) and is characteristic during the prograde metamorphic devolatisation of a pile of pelitic sediments (Norris and Henley, 1976; Goldfarb *et al.*, 1988; Powell *et al.*, 1991). On the other hand similar fluid composition may be attained during extension and retrograde metamorphism by influx of meteoric waters, which reequilibrate at depth (Nesbitt, 1992).

A few siderite samples exhibit positive Eu anomalies, which is a fingerprint of crystallisation from a metamorphogenic solution, i.e. fluid equilibration and uptake of excess Eu^{3+} in a 'hot' metamorphic basement (Bau and Möller, 1992). By assuming a mean siderite carbon isotope composition of $\delta^{13}C_{PDB} \geqslant -12‰$, a formation temperature of 300 °C (see discussion above), and HCO_3^- as a dominating dissolved carbon species, the ore forming solution can be calculated to a carbon isotope composition of $\delta^{13}C_{HCO_3^-} \approx -9‰$.

This would correspond to a deep crustal fluid (Zheng, 1991). However, CO_2 is detected in fluid inclusions and has to be considered as dominating dissolved carbon species. The calculated carbon isotope composition of the fluid of $\delta^{13}C_{CO_2} \approx -15‰$ suggests an uptake of 'organic' carbon. Fluid interaction with black shales and isotopic homogenisation during high-temperature metamorphism are considered most probable, since dark bituminous shales are widespread in the pre-Devonian series of the Rhenohercynian belt (Franke, 1989).

Structural arguments as well as *P–T* estimates delimit siderite mineralisation to the transitional stage from final overall compressive deformation to intial late-kinematic extension, i.e. close to, or

immediately after the peak of metamorphism. Therefore, it can be concluded that prograde devolatisation best explains the origin and composition of the ore forming fluids and the geochemical characteristics of siderite.

The siderite stage as part of the Variscan vein mineralisation. A similar set of data, as presented throughout this paper, does not exist for the other stages of Variscan vein mineralisation except microthermometric results which are summarised by Hein and Behr (1991*a*). Recently published data (Redecke, 1992) fit into the reported ranges (Table 3).

Early stage fluids are of low salinity. Homogenisation temperatures in the range of 205–285 °C point to formation temperatures higher than those for the siderite stage, which is in agreement with paragenetic arsenopyrite (Fig. 2). The latter cannot be applied as a geothermometer (Kretschmar and Scott, 1976) because of its Co-contents in the percent range (Fenchel *et al.*, 1985).

Sulphide stage fluids exhibit a more complex chemical composition than those of the main stage. Formation temperatures and pressures—as obtained from the intercept of cogenetic aqueous and CO_2 inclusions (see above)—are below conditions of siderite precipitation. Pb-isotope data of sulphide stage galena and sulphosalts show little variation over the Rhenish Massif, suggesting Pb-mobilisation from a large-scale homogeneous crustal source (Krahn, 1988; Bielicki and Tischendorf, 1991) by a homogeneous fluid system. The trend of increasing fluid salinity with falling temperatures (Fig. 3) can be explained by retrograde fluid–rock interaction (Bennett and Barker, 1992). Additionally, growth zoning, which is not observed in main-stage minerals, points to possible mixing of deep-seated metal-rich fluids with formation waters (Hein and Behr, 1991*a*).

Rejuvenation stage fluids clearly differ from the preceeding development. Salinity is low (<5% wt.% NaCl equiv.) and temperatures increase from 120 °C (early baryte) to 340 °C (quartz 5; Erlinghagen, 1989). In the Siegerland district the paragenesis (Fig. 2) reflects a drastic change of the mineralising fluids to higher oxygen fugicity. Local intensive fluid–mineral interaction is documented by hematitisation of siderite in the Siegerland or by the occurrence of low-density N_2-rich gaseous inclusions (Hein and Görke, unpubl.), which are only observed in quartz veins hosted by Lower Devonian acid tuffites of the Hunsrück–Lahn district.

By their structural characteristics (see above), their fluid composition and origin, and their *P–T* development (Table 3) *early-*, *main-*, and *sulphide stage* mineralisation fit into the tectonothermal history of the Rhenish Massif (Oncken, 1987). They are classified as *metamorphogenic*. The rejuvenation stage is correlated with the period of enhanced postkinematic heat flow in the Rhenohercynian which is documented by Upper Carboniferous/Lower Permian granite intrusions in the Harz Mountains or by succeeding Lower Permian volcanism (Saar–Nahe basin) at the southeastern margin of the Rhenish Massif.

Acknowledgements

The investigations have been supported financially by the German Research Foundation within the scope of the project 'Tectonic Brines' as part of the central program 'Intraformational Ore Deposition'. The author is indebted to Prof. Dr. H. J. Behr, Göttingen, for supervising this project and is grateful to Prof. Dr. J. Hoefs, Göttingen, and Prof. Dr. P. Möller, Berlin, for critical remarks. M. Bau, P. Dulski, K. P. Erlinghagen, W. Fielitz, J. Gerler, H. Hannak, A. M. van den Kerkhof, V. Lüders, H.-G. Mittmayer, O. Oncken, P. Redecke, Chr. Reé, Chr. Reutel, N. Schneider, G. Schnorrer-Köhler, K. Schürmann, M. Thünker, and Y. Zheng have contributed to this paper, each in his own field and individual way. Two anonymous reviewers helped to improve an earlier version of the manuscript.

Table 3: Structural characteristics, fluid inclusion data, and age determinations of the Variscan vein mineralization in the Rhenish Massif.

Stage	Early[1]	Main (-Siderite)	Sulphide[1]	Rejuvenation[1]
deformation	pre- to syn-kinematic	synkinematic compressive	syn- to late-kinematic	postkinematic
chemical composition salinity (NaCl equiv.) formation temperature estimated pressure gases	Na-Cl < 5 wt. % (205-285)[2]	Na(-K-Fe)-Cl < 5 wt. % 220-320°C 0,7-1,4 Kbar CO_2 (undersaturated)	Na(-K-Fe-Mg-Ca)-Cl < 5 - 18 wt. % 150-250°C 500-800 bar CO_2	Na-Cl < 5 Gew. % 120-340°C < 500 bar N_2 - CO_2
age	----	310/316±10 Ma[3] (K/Ar, metamorphism)	290 ± 9 Ma (Rb/Sr)[3] 305/302±10 Ma (K/Ar) (metamorphism)	270 ± 9 Ma[4] (K/Ar, fault gouge clay)

[1] Compilation after Hein and Behr (1991a). [2] Homogenization temperatures. [3] Ahrendt et al. (1983). [4] Ahrendt and Hein, unpubl.

Finally, the author wishes to express his gratitude to A. J. Barker, Southampton, for his editorial support.

References

Ahrent, H., Clauer, N., Hunziker, J. C., and Weber, K. (1983) Migration of folding and metamorphism in the Rheinische Schiefergebirge deduced from K–Ar and Rb–Sr age determinations. In *Intracontinental Fold Belts* (H. Martin and F. W. Eder, eds.), Springer, Berlin–Heidelberg, 323–38.

Anderle, H.-J., Massone, H.-J., St., Oncken, O., and Weber, K. (1990) Southern Taunus Mountains. In *IGCP 233, Conference on Paleozoic Orogens in Central Europe—Geology and Geophysics, Field Guide Mid-German Crystalline Rise & Rheinisches Schiefergebirge* (W. Franke and K. Weber, eds.), Göttingen–Giessen, 125–48.

Bau, M. (1991) Rare-earth element mobility during hydrothermal and metamorphic fluid–rock interaction and the significance of the oxidation state of europium. *Chem. Geol.*, **93**, 219–30.

—— and Möller, P. (1992) Rare earth element fractionation in metamorphogenic hydrothermal calcite, magnesite and siderite. *Mineral. Petrol.*, **45**, 231–46.

Bauer, G., Ebert, A., von Kamp, H., Müller, D., Pietzner, H., and Scherp, A. (1979) Die Blei-Zink-Erzlagerstätten von Ramsbeck und Umgebung. Monogr. dt. Blei-Zink-Erzlagerst. 6, *Geol. Jahrb.*, **D33**, 1–375.

Behr, H. J. (1989) Die geologische Aktivität von Krustenfluiden. *Nds. Akad. Geowiss. Veröfftl.*, **1**, 4–75.

Bennett, D. G. and Barker, A. J. (1992) High salinity fluids: The result of retrograde metamorphism in thrust zones. *Geochim. Cosmochim. Acta*, **56**, 81–95.

Bielicki, K.-H. and Tischendorf, G. (1991) Lead isotope and Pb–Pb model age determination of ores from Central Europe and their metallogenetic interpretation. *Contrib. Mineral. Petrol.*, **106**, 440–61.

Belss, M. J. M., Bouckeart, J., and Paproth, E. (1989) The Dinant nappes: A model of tensional listric faulting inverted into compressional folding and thrusting. *Bull. Soc. Belg. Geol.*, **98–2**, 221–30.

Bois, C. and ECORS Scientific Party (1988) Major crustal features disclosed by the ECORS deep seismic profiles. *Ann. Soc. géol. Belg.*, **111**, 257–77.

Bornhardt, W. (1910/12) Über die Gangverhältnisse des Siegerlandes und seiner Umgebung. *Arch. Lagerstätt. Forsch.*, **2**, 1–415; **8**, 1–515.

Bouckaert, J., Forck, W., and Vandenberge, N. (1988) First results of the Belgian Geotraverse 1986 (BELCORP). *Ann. Soc. géol. Belg.*, **111**, 279–90.

Buntebarth, G., Koppe, I., and Teichmüller, M. (1982) Paleogeothermics in the Ruhr basin. In *Geothermics and Geothermal Energy* (V. Cermak and R. Hänel, eds.), Schweizerbath, Stuttgart, 45–55.

Cathelineau, M. (1988) Cation site occupancy in chlorites and illites as a function of temperature. *Clay Minerals*, **23**, 471–85.

—— and Nieva, D. (1985) A chlorite solid solution geothermometer. The Los Azufres (Mexico) geothermal system. *Contrib. Mineral. Petrol.*, **91**, 235–44.

Dulski, P. (1992) Determination of minor and trace elements in four Canadian iron-formation standard samples FeR-1, FeR2, FeR3 and FeR4 by INAA and ICP-MS. *Geostandards Newsletter*, **16/2**, 325–32.

Erlinghagen, K.-P. (1989) Fluid inclusion studies of siderite lodes of the Siegerland–Wied District (Rheinisches Schiefergebirge), FRG. *Neues Jahrb. Mineral., Mh.*, 557–67.

Eyssen, G. (1985) Mineralogie und Geochemie von Chloriten des Lahn–Gebietes, südliches Rheinisches Schiefergebirge. *Clausthaler Geowiss. Diss.*, **17**, 1–184, Clausthal-Zellerfeld.

Fenchel, W., Gies, H., Gleichmann, H.-D., Helmind, W., Hentschel, H., Heyl, K. E., Hüttenhain, H., Langenbach, U., Lippert, H.-J., Luznat, M., Meyer, W., Pahl, A., Rao, M. S., Reichenbach, R., Stadler, G., Vogler, H., and Walther, H. W. (1985) Die Sideriterzgänge im Siegerland-Wied-Distrikt.-Sammelwerk dt. Eisenerzlagerst., I *Eisenerze im Grundgebirge*, 1, **D77**, 1–517.

Franke, W. (1989) Tectonostratigraphic units in the Variscan belt of Central Europe. In *Terranes in the Circum-Atlantic Paleozoic Orogens* (R. D. Dallmeyer, ed.), *Geol. Soc. Amer. Spec. Pap.*, **230**, 67–90.

——Bortfield, R. K., Brix, M., Drozdzewski, G., Dürbaum, H. J., Giese, P., Janoth, W., Jödicke, H., Reichert, Cr., Scherp, A., Schmoll, J., Thomas, R., Thünker, M., Weber, K., Weisner, M. G., and Wong, H. K. (1990) Crustal structure of the Rhenish Massif: results of deep seismic reflection lines DEKORP-2 North and DEKORP 2-North-Q. *Geol. Rdsch.*, **79/3**, 523–66.

Fransolet, A.-M., Kramm, U., and Schreyer, W., (1977) Metamorphose und Magmatismus im Venn-Stavelot Massiv, Ardennen. *Fortschr. Mineral.*, **55**, Beih. 2, 75–103.

French, B. M. (1971) Stability relations of siderite ($FeCO_3$) in the system Fe–C–O. *Am. J. Sci.*, **271**, 37–78.

Frost, R. (1979*a*) Mineral equilibria involving mixed-volatiles in a C–O–H fluid phase: The stabilities of graphite and siderite Ibid., **279**, 1033–59.

——(1979*b*) Metamorphism of iron-formation: Parageneses in the system Fe–Si–C–O–H. *Econ. Geol.*, **74**, 775–85.

Gerler, J. (1990) *Geochemische Untersuchungen an hydrothermalen, metamorphen, granitischen und pegmatitischen Quarzen und deren Flüssigkeitseinschlüssen.* Dissertation, 1–169, Universität Göttingen.

Goldfarb, R. J., Leach, D. L., Pickthorn, W. J., and Paterson, C. J. (1988) Origin of lode-gold deposits of the Juneau gold belt, southeastern Alaska. *Geology*, **16**, 440–43.

Hannak, W. (1964) Ergebnisse von Untersuchungen im Blei-Zink-Erzbezirk des südlichen Rheinischen Schiefergebirges. *Erzmetall*, **17**, 291–98.

——(1965) Verteilung von Fe, Mn, Ca und Mg im Karbonspat I der Blei-Zink-Erzgänge des südlichen Rheinischen Schiefergebirges. *Geol. Rdsch.*, **55**, 385–98.

——and Gundlach, H. (1967) Elementverteilung in Karbonspäten der Blei-Zink-Erzgänge des südlichen Rheinischen Schiefergebirges. *Neues Jahrb. Mineral., Abh.*, **107**, 1–20, Stuttgart.

Haskin, M. A. and Haskin, L. A. (1966) Rare earths in European shales: a redetermination. *Science*, **154**, 507–9.

Hein, U. F. and H. Behr (1991*a*) Synorogene Verezungen der variskischen Externiden Mitteleuropas. In SPP *'Intraformationale Lagerstättenbildung', Report 2* (G. Friedrich, ed.), Deutsche Forschungsgemeinschaft, Bonn, 165–73.

——(1991*b*) Synorogenic ore deposition in the Variscan external belt of Europe: A tectonic brine model. In *Source, Transport and Deposition of Metals* (Pagel, M. and Leroy, J. L. eds.), Balkema, Rotterdam, 57–60.

Heinrich, W., Franz, L., Hein, U. F, and Herms, P. (1992) Synthetische Flüssigkeitseinschlüsse als Mikrothermometriestandards: Daten verschiedener Laboratorien mit unterschiedlichen Heiz-Kühl-Systemen im Vergleich. *Ber. d. Deutsch. Mineral. Ges., Beih. z. Eur. Journ Mineral*, **4/1**, 116.

Herbst, F. and Müller, H.-G. (1966) *Der Blei-Zinkerzbergbau im Hunsrück-Gebiet*. Gewerkschaft Mercur, Bad Ems, 1–68.

Hofmann, N. (1990) Zur Paläodynamischen Entwicklung des Präzechsteins in der Norddeutschen Senke. *Nds. Akad. Geowiss. Veröfftl.*, **4**, 5–18.

Jowett, E. C. (1991) Fitting iron and magnesium into the hydrothermal chlorite geothermometer. GAC-MAC Joint Annual Meeting, Program with abstracts, **16**, A62.

Jux, E. (1982) *Petrographische und geochemische Untersuchungen an Gesteinen des Bensberg Engelskirchener Erzreviers*. Dissertation, 1–232, Universität Köln.

Käselitz, L. (1988) *Der mineralogische und geochemische Aufbau des Kniestkörpers im Liegenden der Erzlagerstätte Rammelsberg bei Goslar/Harz*, Dissertation, 1–242, Techn. Univ. Clausthal–Zellerfeld.

Krahn, L. (1988) *Buntmetall-Vererzung und Blei-Isotopie im Linksrheinischen Schiefergebirge*. Dissertation, 1–199, RWTH Aachen.

Kretschmar, U. and Scott, S. D. (1976) Phase relations involving arsenopyrite in the system Fe–As–S and their application. *Canad. Mineral.*, **14**, 364–86.

Lehmann, H. and Pietzner, H. (1970) Der Lüderich-Gangzug und das Gangvorkommen Nikolaus-Phönix im Bergischen Land. *Fortschr. Geol. Rheinld. Westf.*, **17**, 589–664.

Lüders V. and Möller, P. (1992) Fluid evolution and ore deposition in the Harz mountains. *Eur. J. Mineral.*, **4**, 1053–68.

Meisl, S. (1970) Petrographische Studien im Grenzbereich Diagenese-Metamorphose. *Abh. hess. L.-A. Bodenforsch.*, **57**, 1–93.

Möller, P. (1983) Lanthanoids as a geochemical probe and problems in lanthanoid geochemistry—Distribution and behavior of lanthanoids in non-magmatic phases. In *Systematics and properties of the lanthanides* (S. P. Sinha, ed.), NATO ASI series, **C109**, 561–616.

Morgan, J. W. and Wandless, G. A. (1980) Rare earth elements in some hydrothermal minerals: evidence for crystallographic control. *Geochim. Cosmochim. Acta*, **44**, 973–80.

Nesbitt, B. E. (1992) Orogeny, crustal hydrogeology and the generation of epigenetic ore deposits in the Canadian Cordillera. *Mineral. Petrol.*, **45**, 153–79.

Norris, R. J. and Henly, R. W. (1976) Dewatering of a metamorphic pile. *Geology*, **4**, 333–6.

Oncken, O. (1987) Heat flow and kinematics of the Rhenish Basin. In *The Rhenisch Massif: Structure, Evolution, Mineral Deposits and Present Geodynamics* (A. Vogel, H. Miller and R. Greiling, eds.), Viehweg, Mainz, 63–78.

——(1993) Passive margin-continental arc collision, the case of the Rhenohercynian and Saxothuringian zones. *Terra Nostra*, 27.

Powell, R., Will, T. M., and Phillips, G. N. (1991) Metamorphism in Archean greenstone belts: calculated fluid compositions for gold mineralisation. *J. Metam. Geol.*, **9**, 141–50.

Redecke, P. (1992) Zur Geochemie und Genese variszischer und postvariszischer Buntmetallmineralisation in der Nordeifel und der Niederrheinischen Bucht. *Mitteilungen zur Mineralogie und Lagerstättenkunde*, **41**, 1–152, Aachen.

Schulz-Dobrick, B. and Wedepohl, K.–H. (1983) The chemical composition of sedimentary deposits in the Rhenohercynian belt of Central Europe. In *Intracontinental fold belts* (H. Martin and F. W. Eder, eds.), Springer, Berlin–Heidelberg, 211–30.

Schwartz, M. O. and Suronjo (1990) Greizenisation and albitisation at the Tikus tin–tungsten deposit, Belitung, Indonesia. *Econ. Geol.*, **65**, 691–713.

Stahl, W. (1971) Isotopen-Analysen an Carbonaten und Kohlendioxid–Proben aus dem Einflußbereich und der weiteren Umgebung des Brahmscher Intrusivs und an hydrothermalen Carbonaten aus dem Siegerland. *Fortschr. Geol. Rheinld. Westf.*, **18**, 429–38.

Tröger, W. E. and Trochim, H. D. (1966) In *Optische Bestimmung der gesteinsbildenden Minerale* (W. E. Tröger, ed.), Teil 2, Textband, 556–63.

Vogtmann-Becker, J. (1990) Mobilisation und Austausch von Elementen durch Regionalmetamorphose in kambro-ordovizischen Sedimentgesteinen des Stavelot-Venn-Massivs. *Mitteilungen zur Mineralogie und Lagerstättenkunde*, **34**, 1–179, Aachen.

Walshe, J. L. (1986) A six-component chlorite solid solution model and the conditions of chlorite formation in hydrothermal and geothermal systems. *Econ. Geol.*, **81**, 681–703.

Walther, H. W. (1986) Federal Republic of Germany. In *Mineral Deposits of Europe* (F. W. Dunning *et al.*). Vol. 3, Central Europe, Inst. Min. Metal and Min. Soc., London, 175–301.

Walter, J. (1981) *Fluide Einschlüsse im Apatit des Carbonatits vom Kaiserstuhl (Oberrheingraben): Ein Beitrag zur Interpretation der Carbonatitgenese*. Dissertation, 1–188, Univ. Karlsruhe.

Weber, K. (1981) The structural development of the Rheinisches Schiefergebirge. *Geologie en Mijnbouw*, **60**, 149–59.

Wettig, E. (1974) Die Erzgänge des nördlichen, rechtsrheinischen Schiefergebirges, ihr Inhalt und ihre tektonischen Zusammenhänge. *Clausthaler Geol. Abh.*, **19**, 1–363.

Zak, K. and Dobes, P. (1991) Stable isotopes and fluid inclusions in hydrothermal deposits: The Pribram ore region. *Rozpr. Ceskoslovenske Akad. Ved*, Academia, Praha, 3–109.

Zheng, Yong-Fei (1991) *C-, O- und S-Isotopengeochemische Untersuchungen an hydrothermalen Lagerstätten des Harzes*. Dissertation, 1–130, Univ. Göttingen.

[*Manuscript received 4 October 1992: revised 8 March 1993*]